Article:
Hussein, AT, Alresheedi, MT and Elmirghani, MH (2016) Fast and Efficient Adaptation Techniques for Visible Light Communication Systems. IEEE/OSA Journal of Optical Communications and Networking, 8 (6). pp. 382-397. ISSN 1943-0620

https://doi.org/10.1364/JOCN.8.000382

Fast and Efficient Adaptation Techniques for Visible Light Communication Systems

Ahmed Taha Hussein, Mohammed T. Alresheedi and Jaafar M. H. Elmirghani

Abstract— Beam steering visible light communication (VLC) system has been shown to offer performance enhancements over traditional VLC systems. However, an increase in the computational cost is incurred. In this paper, we introduce fast computer generated holograms (FCGHs) to speed up the adaptation process. The new, fast and efficient fully adaptive VLC system can improve the receiver signal to noise ratio (SNR) and reduce the required time to estimate the position of the VLC receiver. It can also adapt to environmental changes, providing a robust link against signal blockage and shadowing. In addition, an angle diversity receiver (ADR) and a delay adaptation technique are used to reduce the effect of inter symbol interference (ISI) and multipath dispersion. Significant enhancements in the SNR, with VLC channel bandwidths of more than 26 GHz are obtained, resulting in a compact impulse response and a VLC system that is able to achieve higher data rates (25 Gbps) with full mobility in the considered realistic indoor environment.

***Index Terms*— Beam Steering, angle diversity receiver, fast computer generated hologram, delay adaptation technique, SNR.**

I. INTRODUCTION

Traditional radio and microwave communication systems suffer from limited channel capacity due to the limited radio spectrum available, while the data rates requested by the users continue to increase exponentially. Achieving very high data rates (multi gigabits per second) using the relatively narrow bandwidth of microwave and millimetre wave systems is challenging [1].

According to a GreenTouch research study, mobile Internet traffic over this decade (2010-2020) is expected to increase by 150 times [2]. Given this expectation of dramatically growing demand for data rates, the quest is already underway for alternative spectrum bands beyond microwaves and millimetre waves. Different technology candidates have entered the race to provide ultra-fast wireless communication systems for users. Visible light communication (VLC) systems are among the promising solutions to the bandwidth limitation problem faced by microwave systems [1]. They are also considered among the potential candidates for 5G indoor systems [3]. Over the last decade, there has been increased interest in VLC due to its potential to achieve high data rates and its use of inexpensive and energy efficient light emitting diodes (LEDs) and optoelectronic devices [1]. However, the main challenges hindering the development of a VLC system are the low modulation bandwidth of the LEDs and inter symbol interference (ISI). The modulation bandwidth available in the transmitters (LEDs) is typically less than the VLC channel bandwidth, which means that the former typically limits the transmission rates. Therefore, alternative transmitters are needed for VLC systems to achieve high data rates. The typical peak data rate achieved by using commercial RGB LEDs with low complexity modulation (on off keying, OOK) is up to 500 Mbps [4]. Recently, a 3 Gbps VLC system based on a single µLED using orthogonal frequency division multiplexing (OFDM) has been successfully demonstrated [5]. The highest throughput achieved by LEDs to the best of our knowledge was reported in [6], where the aggregate throughput was 4.5 Gbps when using carrier-less amplitude and phase (CAP) modulation and recursive least squares (RLS) based adaptive equalization, wavelength division multiplexing (WDM) and RGB LEDs. The design and implementation complexity are a major concern in these systems.

Beam steering has been widely investigated in communication systems to maximise the SNR at the receiver [7], [8]. Therefore, beam steering can be an attractive option to consider in VLC systems to enhance the system performance. Recently, transmission beam steering for multi input multi output (MIMO) infrared optical wireless (IROW) systems with intensity modulation and direct detection has been developed [9]. In addition, recent work has demonstrated optical wireless energy transmission using optical beam steering and beam forming with a spatial light modulator (SLM). They focused light on the desired target using optical beam steering and beam forming to transfer optical wireless energy [10].

A VLC beam steering array can be constructed using electronically controlled mirrors in front of the receiver. An inexpensive approach that can be used to provide good link

Manuscript received November 5, 2015.

A. T. Hussein is with the School of Electronic and Electrical Engineering, University of Leeds, Leeds LS2 9JT, U.K. (e-mail: ml12ath@leeds.ac.uk).

Mohammed T. Alresheedi is with the Department of Electrical Engineering, King Saud University, Riyadh, Saudi Arabia (e-mail: malresheedi@ksu.edu.sa).

J. M. H. Elmirghani is with the School of Electronic and Electrical Engineering, University of Leeds, Leeds LS2 9JT, U.K. (e-mail: j.m.h.elmirghani@leeds.ac.uk).

quality during mobility is to use mirrors with piezoelectric actuators in front of the receiver [11], [12]. Another approach is the tilting of the transmitter and receiver together using piezoelectric actuators that are controlled electronically. As with the mirror method, the tilting method also needs to be controlled by an electronic circuit. However, these methods lead to a bulky receiver that cannot be used for mobile devices and can only be used in low transmission rate stationary systems, up to 100 Mbps shown in [11], [12].

Previous work has shown that significant enhancements in the VLC system data rates can be achieved by replacing LEDs with LDs coupled with the use of an imaging receiver instead of the conventional wide field of view (FOV) receiver [13], [14], [15]. A data rate of 10 Gbps in a realistic environment has been shown to be possible with a VLC system when a delay adaptation technique in conjunction with laser diodes and imaging receiver were used with a simple modulation format (OOK) and without the use of relatively complex wavelength division multiplexing approaches [13]. Significant improvements were shown to be possible when a VLC relay assisted system is combined with an imaging receiver and a delay adaptation technique [16]. However given typical parameters, the latter system cannot provide a throughput beyond 10 Gbps due to its low signal to noise ratio (SNR). Recently, beam steering has been proposed in VLC systems to maximise the SNR at the receiver [17]. Simulation results have shown that a significant improvement in the data rate (20 Gbps for a stationary user and 14 Gbps for a mobile user) can be achieved in a mobile VLC system that employs beam steering. The improvements achieved are however at the cost of complex adaptation requirements. The complexity is associated with the computation time required to identify the optimum location to steer the beam to, as well as the time needed to generate the hologram that generates beams at the optimum angles.

The work presented in this paper aims to address the impairments of VLC systems and provide practical solutions, hence achieving data rates beyond those reported in [13]-[17]. In this paper, for the first time to the best of our knowledge, we report the use of holograms and beam steering in VLC systems with efficient adaptation. The data rates achieved by our proposed system, i.e. 25 Gbps for a stationary user and 22.2 Gbps for a mobile user, are the highest data rates to date for an indoor VLC system with simple modulation format (OOK) and without the use of relatively complex wavelength division multiplexing approaches, to the best of our knowledge. We introduce new fast computer generated holograms (FCGHs) for beam steering making use of simulated annealing optimization. The holograms are pre-calculated and stored in the proposed system (each is suited for a given (range of) transmitter and receiver locations) and eliminate the need to calculate holograms real time at each transmitter and receiver location. The concept of finite computer generated holograms has been recently proposed in VLC system [17]. The work in [17] investigated a very limited case of finite pre-stored holograms and studied it in a realistic indoor environment to examine the impact of shadowing. Here we extend the work in [17] by (i) introducing FCGHs, (ii) studying the VLC system complexity and SNR penalty, (iii) employing angle diversity receiver with narrow FOVs, (iv) evaluating a high data rate system (25 Gbps), and (v) considering a real environment that experiences shadowing to assess the utility of FCGHs.

In this study the RGB-LDs light unit is followed by the SLM that generates beams whose locations can be varied where the transmission angles θ_x and θ_y in the xy axes are varied between -70° and 70° (half power beam angle of RGB-LDs light unit was 70°) with respect to the transmitter's normal in both the x and the y (α_{-x} to α_x and α_{-y} to α_y) directions respectively.

Recently, we proposed the use of an angle diversity receiver (ADR) for a VLC system to provide a robust link and mitigate multipath dispersion, as well as to improve the overall system performance [14]. In this study we used an ADR with selective combining to choose the best branch. A delay adaptation technique (DAT) for a VLC system was proposed in [13] and it is used here as it is shown to offer channel bandwidths of more than 26 GHz (in a worst case scenario), which enables the VLC system to operate at data rates of more than 25 Gbps. The adaptation techniques (FCGHs and DAT) require repetitive training and a feedback channel from the receiver to transmitter at a low data rate. An infrared (IR) diffuse channel is suggested to realize this link. The ultimate goal of this study is to enhance the 3 dB channel bandwidth, minimize the impact of ISI, and increase the SNR when the VLC system operates at a high bit rate of 25 Gbps under the effect of multipath dispersion, shadowing, mobility and receiver noise.

The VLC room setup and channel characteristics are described in the next Section. The receiver structure is given in Section III. Section IV describes the VLC system configurations and fast computer generated holograms for VLC system. The VLC system complexity is considered in Section V. The impact of beam steering on illumination is investigated in Section VI. The simulation results in an empty room are outlined in Section VII. Robustness against shadowing is evaluated in Section VIII. Finally, conclusions are drawn in Section IX.

II. The VLC Room Setup and Channel Characteristics

In order to study the performance of our proposed system, under mobility and multipath dispersion, consideration was given to an unoccupied rectangular room that had no furnishings, with dimensions of 8 m × 4 m × 3 m (length × width × height), similar to those considered in the previous works [13]-[17]. Previous research in [18] has found that the power reflected by elements on either the wall or the ceiling is Lambertian in nature, having a reflectivity of 0.8 for walls and ceiling, and 0.3 for the floor. In this study, we regarded the reflections from the windows and doors to be identical to those coming from the walls. The reflecting elements can be modelled by subdividing the ceiling and walls into small square surfaces (dA) which operate as secondary small diffuse transmitters (n=1), where n is the Lambertian emission order. The effect of a realistic indoor office (door, windows, physical partitions, chairs, and other objects) will be considered in Section VIII. Surface elements of 5 cm × 5 cm for first-order reflections and 20 cm × 20 cm for second-order reflections were used. These values were selected to keep the computation requirements within a reasonable time (the computation time increases

dramatically when the surface element size is decreased). Previous research considered only LOS and reflections up to a first order [19], [20], [21]. However, this may not provide a full description of the characteristics of the system. Therefore, in this study reflections up to the second order were considered, since the second order reflections can have a great impact on the system performance at multi gigabits per second data rates [21]. Reflections can continue beyond second-order, however it is noted that the power received from the third-order reflections for the VLC systems is extremely low compared to LOS, first-order, and second-order reflections [16]. Therefore, for convenience, computer analysis up to second-order reflections has been considered in this study.[1]

A combination of red, green and blue lasers with a diffuser can be used to generate white light that has good colour rendering [22]. Therefore, the room's illumination was provided by eight RGB-LD light units which were used to ensure that ISO and European standards were satisfied [23]. Each LD light unit has 9 (3×3) RGB-LD. The LD lights were installed at a height of 3 m above the floor. The specifications of the RGB-LDs used in this study were adapted from the practical results reported in [24], where the measured illuminance for each RGB-LD was 193 lx.

The VLC room with the coordinates of the RGB-LDs light units is shown in Fig. 1. The room's illumination was provided by eight RGB-LDs light units that were used to ensure ISO and European standards were satisfied. Fig. 2 shows the horizontal illumination distributions from the eight RGB-LD light units at the communication floor level. It is clear from this figure that there is sufficient illumination according to EU and ISO standards [23]. The simulations and calculations reported in this study were carried out using MATLAB. Our simulation tool was similar to the one developed by Barry et al. [25]. In our evaluation, the channel characteristics, optical power received, delay spread, 3 dB channel bandwidth and SNR calculations were determined in similar ways to those used in [26], [27], [28]. Additional simulation parameters are given in Table I.

In indoor OW communication systems, intensity modulation with direct detection (IM/DD) is the preferred choice as a result of its reduced cost and complexity [18]. The receiver makes use of a detector that produces a photocurrent $I(t)$ which is proportional to the received instantaneous optical power. The typical detector area contains tens of thousands of very short wavelengths of the received optical signal, and hence allows spatial diversity and prevents fading. The indoor optical wireless IM/DD channel can be completely described via its impulse response $h(t)$. It can be modelled as a linear baseband system [29], given by:

$$I(t, Az, El) = \sum_{m=1}^{M_t} Rx(t) \otimes h_m(t, Az, El) + \sum_{m=1}^{M_t} Rn_m(t, Az, El) \quad (1)$$

where t is the absolute time, El and Az represent the direction of the arrival in elevation and azimuth angles respectively. M_t is the total number of reflecting elements, $x(t)$ is the transmitted instantaneous optical power, $\otimes$ denotes convolution, R is the detector responsivity and $I(t, Az, El)$ is the received photocurrent at a certain location resulting from M_t reflecting surfaces. Lastly, $n_m(t, Az, El)$ represents the background light noise due to m^{th} reflecting elements at the receiver.

The power incident on a reflecting element, either on the walls or ceiling can be modelled by Lambertian model:

$$dp_n = \frac{n+1}{2\pi} \times cos^n v_i \times P_s \times \frac{dA}{D_1^2} cos\beta \quad (2)$$

where P_s is the total average transmitted optical power emitted by the source (LDs), D_1 is the distance between transmitter and element dA, v_i is the incidence angle with respect to the transmitter's surface normal, β is the angle between the surface normal of the element dA and the incident ray, and n is the mode number which describes the shape of transmitted beam. Higher values of n, lead to narrower light beams, and are related to the half power semi-angle (hps) of the transmitter pattern. The Lambertian emission order (n) can be defined as [27]:

$$n = -\frac{ln(2)}{ln(cos(hps))} \quad (3)$$

TABLE I
SIMULATION PARAMETERS

Parameters	Configurations
Length	8m
Width	4m
Height	3m
ρ-ceiling	0.8 [18]
ρ-xz wall	0.8 [18]
ρ-yz wall	0.8 [18]
ρ-xz op-wall	0.8 [18]
ρ-yz op-wall	0.8 [18]
ρ-floor	0.3 [18]
Bounces	1 2
Number of elements	32000 2000
dA	5cm×5cm 20cm×20cm [30], [31]
Transmitters	
Number of transmitters	8
Locations (x, y, z)	(1,1,3), (1,3,3), (1,5,3), (1,7,3) (3,1,3), (3,3,3), (3,5,3), (3,7,3)
Elevation	90°
Azimuth	0°
Number of RGB-LDs in each transmitter unit	9 (3×3)
Semi-angle at half power	70°
Centre luminous intensity	162 cd [24]
Transmitted optical power of a RGB-LDs	2 W [24]

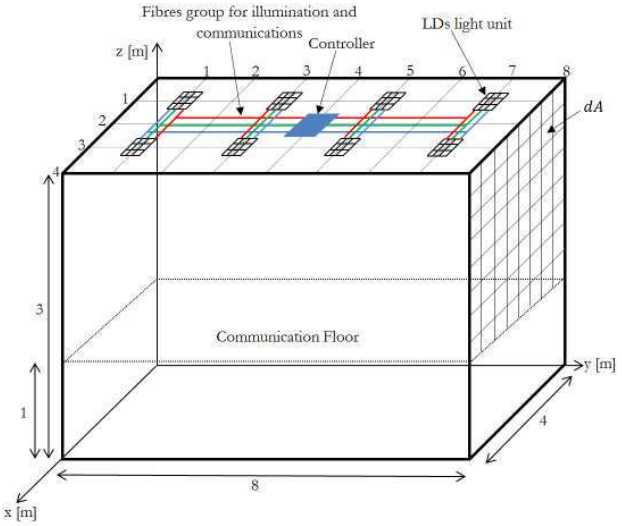

Fig. 1: VLC system room.

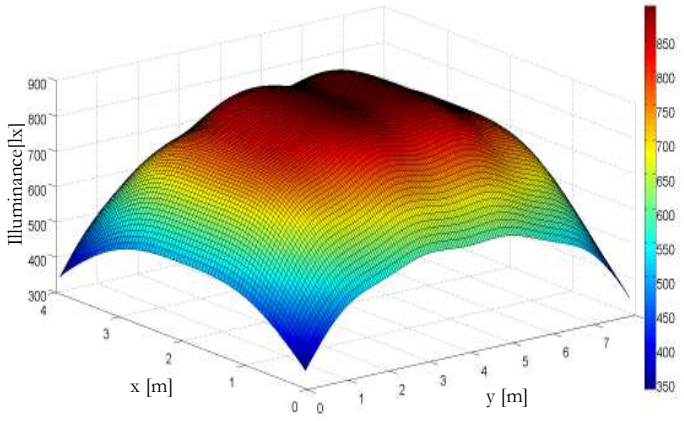

Fig. 2: Distribution of horizontal illumination at the communication floor, Min. 336 lx and Max. 894 lx.

Various parameters can be derived from the simulated impulse response, such as the delay spread and 3 dB channel bandwidth. The delay spread is a good measure of the signal pulse spread due to the temporal dispersion of the incoming signal. The delay spread of an impulse response is given by:

$$D = \sqrt{\frac{\sum(t_i-\mu)^2 P_{ri}^2}{\sum P_{ri}^2}} \quad (4)$$

where t_i is the delay time associated with the received optical power P_{ri} and μ is the mean delay given by:

$$\mu = \frac{\sum t_i P_{ri}^2}{\sum P_{ri}^2} \quad (5)$$

III. Angle Diversity Receiver

In contrast to the single wide FOV receiver, an ADR is a collection of narrow FOV detectors pointed in different directions. The ADR consists of three branches with photodetectors that have a responsivity of 0.4 A/W each. The ADR uses photodetectors with an area of 4 mm^2 each. The ADR was always placed on the communication floor, and results were obtained along the lines x =1 m or x =2 m. The direction of each branch in an ADR is defined by two angles: the azimuth angle (AZ) and the elevation angle (EL). The AZs of the three detectors were set at 0^o, 180^o and 0^o, and the ELs for the three branches were fixed at 90^o, 60^o and 60^o. The corresponding FOVs were fixed to 30^o, 25^o and 25^o. The AZs, ELs and FOVs were chosen through an optimization process to achieve high SNR and low delay spread. The reception angle calculations for any detector in the ADR are given in detail in [16]. Fig. 3 illustrates the physical structure of the ADR. The photocurrents received in each branch can be amplified separately and can be processed using different methods, such as selection combining (SC), equal gain combining (EGC) and maximum ratio combining (MRC), to maximise the power efficiency of the system. For simplicity, SC is considered here in order to process the resulting electrical signals. SC represents a simple form of diversity, where the receiver simply selects the branch with the best SNR.

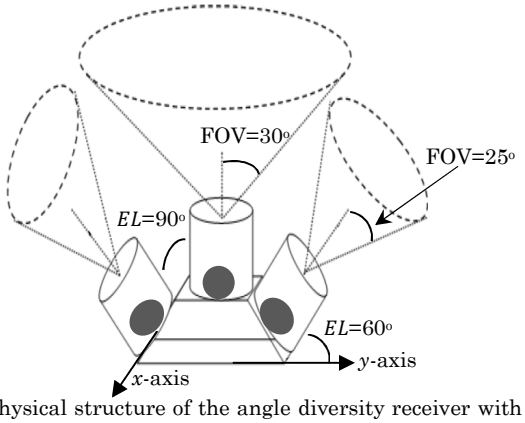

Fig. 3: Physical structure of the angle diversity receiver with three branches.

A simulation package based on a ray-tracing algorithm was developed for arbitrary transmitter-receiver configurations in an arbitrary room size that has diffuse reflectors, in order to compute the impulse response on the entire communication floor [13]-[17]. Additional features were introduced to enable delay adaptation and FCGHs. The received multipath profiles due to each RGB-LDs were computed at each photodetector, based on the detector's FOV and the area the detector observes at each set of transmitter and receiver locations. The resultant power profile at each photodetector is the sum of the powers due to the total number of RGB-LDs seen by each branch.

IV. VLC Systems' Configurations

In this section, two VLC systems are presented, analyzed and compared to identify the most appropriate system for use in high-speed VLC systems (25 Gbps and beyond).

A. DAT ADR LDs-VLC system

The DAT ADR LDs-VLC system employed eight RGB-LDs transmitters (lighting fixtures) on the ceiling connected by fibre interconnect and controlled by a central controller and an ADR with three branches. The delay adaptation technique (DAT) is combined with ADR LDs-VLC (DAT ADR LDs-VLC) to enhance the overall system performance. The DAT ADR LDs-VLC system was previously proposed in [14], [15] and it is considered here to compare it with our new proposed VLC system.

B. Fully adaptive ADR VLC system

The recently proposed beam steering LDs-VLC system has achieved 20 Gbps for stationary user and 14 Gbps for mobile user (the time required for adaptation algorithms during mobility was 296 ms) [17]. However, high complexity is associated with the computation required to identify the optimum beam steering location. In order to solve this problem, we introduce a new FCGHs using simulated annealing to speed up the beam steering process. The holograms are pre-calculated and stored in the proposed system (each hologram is suited for a given (range of) transmitter and receiver locations) and eliminate the need to calculate a real-time hologram at each transmitter and receiver location. In this work the RGB-LDs light unit has

the ability to direct part of the white light towards the receiver location to enhance the SNR when operating at high data rates.

The adaptation algorithms are implemented in a certain RGB-LDs light unit for a single receiver at a given set of positions. When the receiver starts moving, they are applied in another RGB-LDs light unit according to the new receiver location (coordinates). The reduction in complexity and SNR improvement at high data rates (i.e. 25 Gbps) can be achieved according to the following algorithms:-

i. Select the best (STB)

STB algorithm is proposed to locate the closest transmitter (RGB-LDs) to the receiver to implement the fully adaptive ADR VLC system. The STB algorithm identifies the closest transmitter to the receiver according to the following steps:

1- A pilot signal is sent from one of the VLC transmitters.
2- The SNR is estimated at the receiver by branch 1 of the ADR.
3- Repeat step 2 for the other branches in the ADR.
4- Repeat steps 2 and 3 for the other VLC transmitter units.
5- The receiver sends (using an infrared beam) a low data rate control feedback signal to inform the controller of the SNRs associated with each transmitter.
6- The transmitter that yields the best SNR is chosen by the controller (typically the closest transmitter to the receiver in our simulations).

Once the receiver receives the coded signal from the RGB-LDs light unit, the SNR is computed and a feedback signal is sent. If the time taken to calculate the value of each SNR with each RGB-LDs unit is equal to 1 ms (based on typical processor speeds) then the STB algorithm training time is 8 ms (8 RGB-LDs units × 1 ms).

ii. Fast computer generated holograms (FCGHs)

For a large room of 8m × 4m, the communication floor is divided into eight regions (2m × 2m per region). The floor (2 m × 2m) under the visible light sources is subdivided into small areas, for example we divided it to 256 subdivisions (see Fig. 4). In the case of classic beam steering [17] the transmitter first sequentially tries all m holograms (256 holograms in this case) and the receiver computes the SNR associated with each hologram at the receiver and relays this information to the transmitter for the transmitter to identify the best hologram to use (update the holograms). This is an exhaustive search mechanism among the stored holograms. If each SNR computation is carried out in 1 ms (based on typical processor) then the total adaptation time when the receiver moves is 256 ms. A further improvement in SNR can be achieved by increasing the number of regions on the floor which leads to smaller regions and improved SNR, but a larger number of holograms to choose from leading to an increase in the time required to identify the best holograms. For instance, increasing the number of regions from 256 to 512 will lead to an increase in the total number of holograms to 512. Hence the computation time required to identify the optimum holograms is increased to 512 ms. In order to overcome this problem, a FCGHs algorithm is introduced to effectively improve the SNR (through the use of more holograms) while reducing the computation time required to identify the optimum hologram.

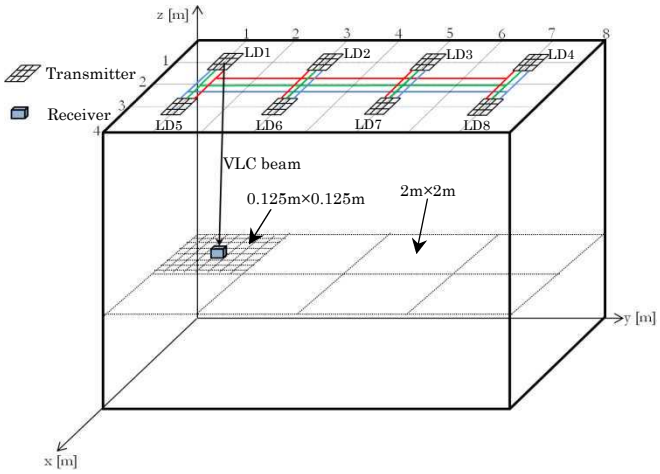

Fig. 4: Architecture of our proposed VLC communication system when the transmitter is placed at (1m, 1m, 3m) and the receiver is on communication floor.

The FCGHs algorithm determines the optimum hologram that yields the best receiver SNR based on a divide and conquer (D&C) algorithm. The transmitter divides the stored holograms into four quadrants with a boundary based on the hologram transmission angles ($-\delta_{min}$ to 0) and (0 to δ_{max}) in both x, y axes. The transmitter first tries the middle hologram at each quadrant (four holograms will be first tried) to identify the sub-optimal quadrant; hence reducing the number of holograms that need to be tried by a factor of 4 in the first step. The receiver sends a feedback signal at a low rate, which informs the transmitter about the SNR associated with each hologram. The hologram that results in the best receiver SNR is identified as a sub-optimum hologram, and the quadrant that includes this sub-optimum hologram will be divided in the next step into four sub-quadrants. The transmitter again scans the middle hologram at four new sub-quadrants and identifies the second sub-optimal hologram; hence identifying the second sub-optimal quadrant. The transmitter again divides the new second sub-optimal quadrant into four quadrants in a similar manner to the first and second sub-optimal quadrants to identify the third sub-optimal quadrant. The quadrant that is represented by the third sub-optimal hologram will be scanned. This technique helps to reduce the computation time required to identify the optimum hologram when a very large number of holograms is used. The proposed FCGHs algorithm can be described for a single transmitter and receiver as follows:

1- The RGB-LDs light unit that has been chosen in the STB algorithm first divides the stored holograms into four main groups associated with quadrants based on the hologram transmission angles. The boundary angles associated with the first quadrant are δ_{max-x} to 0 in the x-axis and δ_{max-y} to 0 in y-axis.
2- The RGB-LDs transmits a pilot signal using the middle hologram in each quadrant in order to determine the first sub-optimum hologram.
3- The SNR is computed at each step (each hologram) and the receiver sends a control feedback signal at a low rate to inform the controller of the SNR

associated with each scan. This feedback channel can be implemented using an infrared beam.

4- The hologram that yield the best SNR is chosen by the controller (identifies sub-optimal quadrant for next iteration).
5- The new scanning area is divided into four quadrants and repeats steps 2 to 4 to identify the second sub-optimal quadrant.
6- Repeat steps 2 to 5 to identify the best location that gives the highest SNR (the divide and conquer process continues and the transmitter determines the optimal hologram transmission angles that maximise the receiver's SNR).

The proposed FCGHs reduce the computation time from 224 ms taken by the classic beam steering LDs-VLC system to 32 ms (32 possible locations should be scanned in all iterations × 1 ms).

The first step is to estimate the receiver location using the FCGHs then the transmitter steers part of RGB-LDs white light to the VLC receiver, which leads to enhanced received SNR. The enhancement in the signal strength by the beam steering approach can improve the transmission distance. It should be noted that, FCGHs and beam steering were implemented in a certain light unit (see Fig.4); when the receiver starts moving, they are applied in another light unit according to the new receiver location (coordinates).

The beam steering focuses a part of the light of one of the RGB-LDs towards the coordinates that were found by the FCGHs. According to the illumination results, which will be discussed in the Section VI, up to 20% of the RGB-LDs light unit can be beam steered towards the receiver's location while the remaining white light (i.e. 80%) is used for illumination.

It is worth noting that instead of laser beam steering, indeed multiple lasers can be mounted at the transmitter with given beam profiles so that each laser can cover part of the environment. This design can be simpler and more efficient than beam steering provided it is able to strike a balance between having few beams / lasers for simplicity and having a narrow beam to avoid multipath dispersion while providing full coverage of the environment. We will investigate and optimise this architecture in future work.

SLMs can be attached to each RGB-LD light unit. White light from light unit enters the holographic beam steerer module and it is first collimated. Then the beam passes through a half wave plate and a polarizer to achieve vertical polarization (see Fig.5). This light then illuminates an SLM, which operates in a phase only mode. A blazed grating profile is programmed on the SLM to achieve the beam steering function (this can be carried out by controller). The SLM can generates beams whose locations can be varied where the transmission angles θ_x and θ_y in the xy axes are varied between -70° and 70° (half power beam angle of RGB-LDs light unit was 70°) with respect to the transmitter's normal in both the x and the y (α_{-x} to α_x and α_{-y} to α_y) directions respectively. The SLM produces a single beam and scans it with step angle (β) along a range of rows and columns in the room to identify the location that yields the best receiver SNR based on a divide and conquer (D&C) algorithm (see Fig. 5). The coordinates of this location are used as the centre of the beam direction.

A SLM is a transparent optical device which can modulate light spatially in phase or amplitude in each pixel. Therefore, it can operate as a dynamic diffractive element controlled by electrical signal. With the Fresnel lens function, the SLM can be operated as a dynamic convex lens. The SLM can generate beams to scan communication floor to estimate the receiver location, so that part of the white light can be directed towards a desired target (receiver) using beam steering to improve SNR.

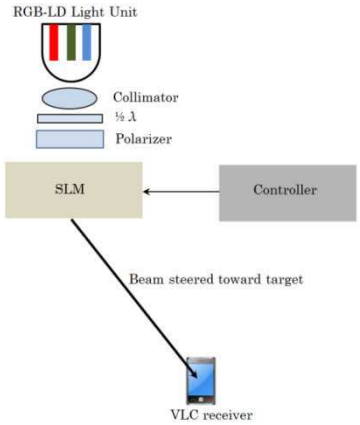

Fig. 5: Beam steering technique applied at one of the RGB-LDs light unit.

iii. Delay adaptation technique (DAT)

It should be noted that the delay spread in a VLC system that is influenced by the RGB-LDs spots' relative positions and the number of RGB-LDs spots seen within the FOV of each detector [13]. Thus, emitting signals from all RGB-LDs units at the same time may cause a time delay differential between the signals received at the pixel, which results in spreading the received pulse and hence limiting the bandwidth. Therefore, instead of sending the signals at the same time from different LD light units, the delay adaptation algorithm sends the signal that has the longest journey first, and then sends the other signals with different differential delays (Δt) so that all the signals reach the receiver at the same time. The delay adaptation algorithm for a VLC system was proposed in [13], and it is used here to offer improvements in terms of system bandwidth. The delay adaptation can be implemented through array elements delayed switching. The delay adaptation adjusts the switching times of the signals as follows:

1- A pilot signal is sent from the first transmitter.
2- The mean delay (μ) at the receiver for the first lighting unit is estimated at the receiver side by branch 1 of the ADR.
3- Repeat step 2 for the other branches in the ADR.
4- Repeat steps 2 and 3 for the other VLC transmitter units.
5- The receiver sends a control feedback signal to inform the controller of the associated delay with each received signal from each transmitter.
6- The controller introduces a differential delay (Δt) between the signals transmitted from the transmitters.
7- The transmitter units send signals according to the delay values, such that a transmitter unit that has

the largest delay, i.e. longest path to the receiver, transmits first.

Indoor users move at a speed of about 1 m/s maximum [32]. We therefore propose that the receiver re-estimates its SNR at the start of a one second frame, and if this has changed compared to the previous frame's value then the receiver uses the feedback channel to update the controller. The MAC protocol should include a repetitive training period to perform the algorithms in Tables II, III and IV. It should be noted that the FCGHs described apply to a single transmitter and a single receiver position. If there is more than a single receiver (multi user) in the room, then a MAC protocol should be used. This will regulate which transmitter-receiver pair can use which resources (for example time slots, code, wavelength) and when. Potential MAC protocols in this environment include carrier sense multiple access (CSMA), packet reservation multiple access and multi-carrier code division multiple access. Furthermore opportunistic scheduling [33] can be employed where the optimum hologram is chosen to maximize the SNR in a given region (set of users) for a given time period. The multi-user system can alternatively select the hologram that optimizes a given performance criterion.

If the time taken to determine the value of each SNR and delay associated with each transmitter (relative to the start of the frame) is equal to 1 ms (based on typical processor speeds), then the STB algorithm, FCGHs and DAT training time will be 112 ms (8 RGB-LDs units × 1 ms + 32 possible locations should be scanned in all iterations × 1 ms + 9 RGB-LDs in each transmitter unit × 8 transmitter units × 1 ms). This time (112 ms, once every one second frame) is sufficient given that adaptation algorithms have to be carried out at the rate at which the environment changes (pedestrian movement). Therefore, the fully adaptive ADR VLC system can achieve 100% of the specified data rate when it is stationary, and 88.9% in the case of user movement, (user or object movement in the room).

TABLE II
STB ALGORITHM

Inputs: N =8; (Number of RGB-LDs light units)
j =3; (Number of branches in ADR)
$p(.)$ is a rectangular pulse over $[0, Tb]$, $Tb = 1/B$ (B is the bit rate).

1. **for** S =1: j;
2. **for** R = 1: N;
3. Calculate and sum the received powers within a time bin (0.01 ns duration)
4. Produce the impulse response $h_j(t)$
5. Calculate the pulse response $h_j(t) \otimes P(t - Tb)$ and then calculate $(PS_1 - PS_0)$
6. Compute $SNR_j = \left(\frac{R(P_{S1} - P_{S0})}{\sigma_t}\right)^2$
7. **end for**
8. $SNR_N = max\ (SNR_j)$
9. **end for**
10. $SNR_{max} = max\ (SNR_N)$
11. Select RGB-LDs unit that yields SNR_{max}

TABLE III
FCGHS ALGORITHM

Inputs: θ_x^{start}=-70° and θ_x^{end}=70° (the lower and higher holograms scan ranges along x-axis).
θ_y^{start}=-70° and θ_y^{end}=70° (the lower and higher holograms scan ranges along y-axis).
θ_{steps}=26.56° (initial value, step size 100 cm)

1. **for** i = 0:26.56:140;
2. **for** l = 0:26.56:140;
3. $\theta_x = i$; $\theta_y = l$; (Transmission angles in x and y axes)
4. Produce a hologram with a direction associated with θ_x and θ_y.
5. **for** S =1: j;
6. Calculate and sum the received powers within a time bin (0.01 ns duration)
7. Produce the impulse response $h_j(t)$
8. Calculate the pulse response $h_j(t) \otimes P(t - Tb)$ and then calculate $(PS_1 - PS_0)$
9. Compute $SNR_j = \left(\frac{R(P_{S1} - P_{S0})}{\sigma_t}\right)^2$;
10. **end for**
11. $SNR\ (i, l) = max\ (SNR_j)$;
12. $detector\ (i, l) = find\ (SNR_j) == (max\ (SNR_j))$;
13. **end for**
14. **end for**
15. $SNR_{max} = max\, SNR\ (i, l)$;
16. $[\theta_{x-sub-optimum}, \theta_{y-sub-optimum}] = find\ (SNR\ (i, l)) == (SNR_{max})$; (identify sub-optimum hologram).
17. **If** $|\theta_{x-sub-optimum}| \leq (|\theta_x^{end}| - |\theta_x^{start}|)/2$ (reset new scan range in the x-axis)
18. $\theta_x^{end} = \theta_{x-sub-optimum}$;
19. **Else**
20. $\theta_x^{start} = \theta_{x-sub-optimum}$;
21. **end If**
22. **If** $|\theta_{y-sub-optimum}| \leq (|\theta_y^{end}| - |\theta_y^{start}|)/2$ (reset new scan range in the y-axis)
23. $\theta_y^{end} = \theta_{y-sub-optimum}$;
24. **Else**
25. $\theta_y^{start} = \theta_{y-sub-optimum}$;
26. **end If**
27. $\theta_x^{optimum} = \theta_{x-\text{sub-optimum}}$; $\theta_y^{optimum} = \theta_{y-\text{sub-optimum}}$; (identify optimum hologram).

TABLE IV
DAT ALGORITHM

1. **for** S =1: j;
2. **for** R =1: N;
3. Compute the impulse response observed by the desired branch.
4. $\mu_{NLD_S} = \frac{\sum_i t_i P_{ri}^2}{\sum_i P_{ri}^2}$; (compute mean delay associated with each signal from each RGB-LDs unit)
5. **end for**
6. **end for**
7. $\mu_{max} = max(\mu_{NLD_S})$;
8. **for** R = 1: N;
9. $\Delta t\_N_{LD} = \mu_{max} - \mu_{NLD_S}$; (Calculate the time delay)
10. Compute the impulse response $h_{NLD}(t)$ observed by the desired branch.
11. Introduce time delay as $h_{NLD}(t - \Delta t\_N_{LD})$; (shift the impulse response)
12. **end for**
13. Produce the optimised impulse response $h_{optimised}(t)$
14. Calculate the pulse response $h_{optimised}(t) \otimes P(t - Tb)$ and then calculate $(PS_1 - PS_0)$
15. Compute the delay spread, 3dB channel and SNR optimised.

The concept of finite computer generated holograms has been recently proposed in VLC system [17] and it is developed here to speed up the adaptation process in the proposed VLC system. Evaluation of phase and pattern distribution were determined in similar ways to those used in [17]. Fig. 6 shows four snapshots of the hologram reconstruction intensity at the far field and phase distributions. When the number of iterations increases, the reconstruction intensities are improved. This is attributed to the use of simulated annealing which attempts to reduce the cost function, hence improving phases in the constructed hologram. Fig.7 shows the desired spots' intensities in the far field. The cost function versus the number of iterations completed is shown in Fig. 8.

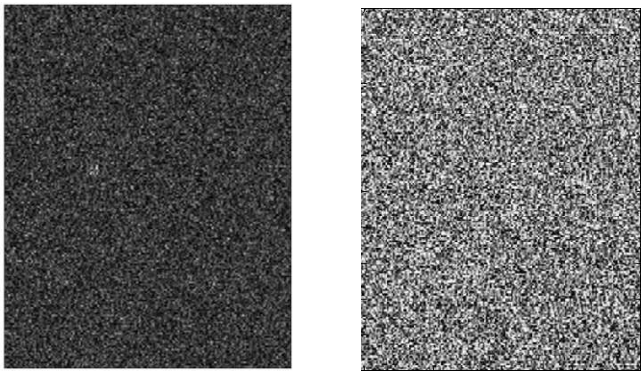

Reconstruction Intensity Hologram Phase

Iteration 1

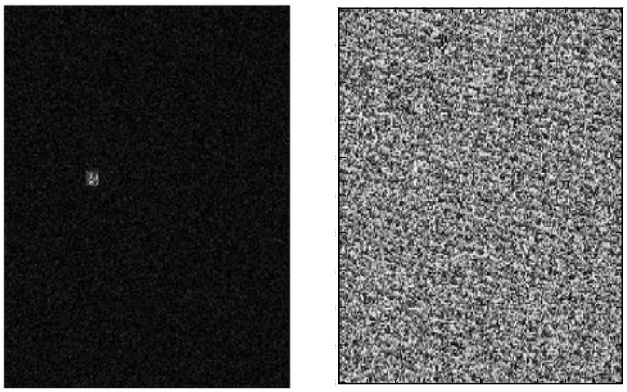

Reconstruction Intensity Hologram Phase

Iteration 5

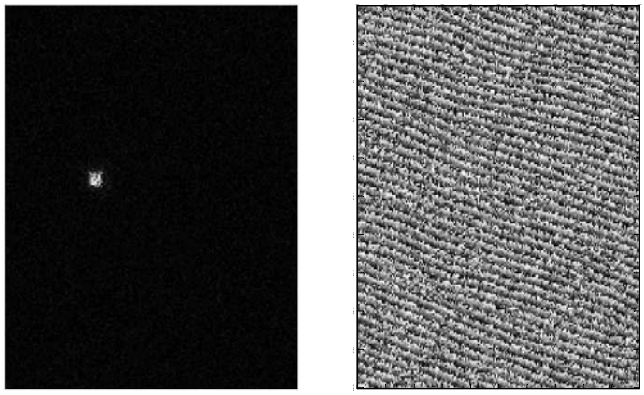

Reconstruction Intensity Hologram Phase

Iteration 15

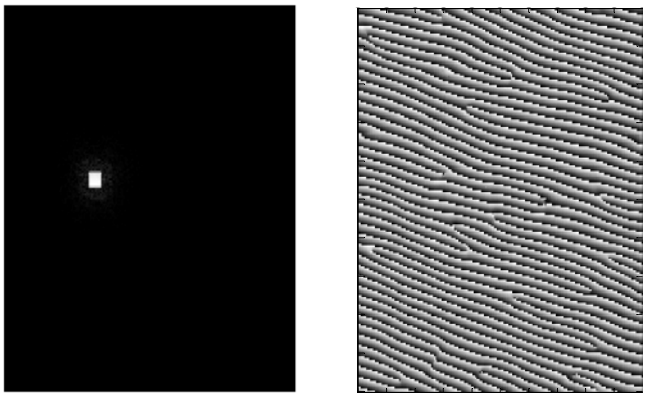

Reconstruction Intensity Hologram Phase

Iteration 100

Fig. 6: The reconstruction intensity at the far field and hologram phase pattern at iterations 1, 5, 15 and 100 using simulated annealing optimisation. Different gray levels represent different phase levels ranging from 0 (black) to 2π (white).

Fig. 7: The desired spots intensity in the far field.

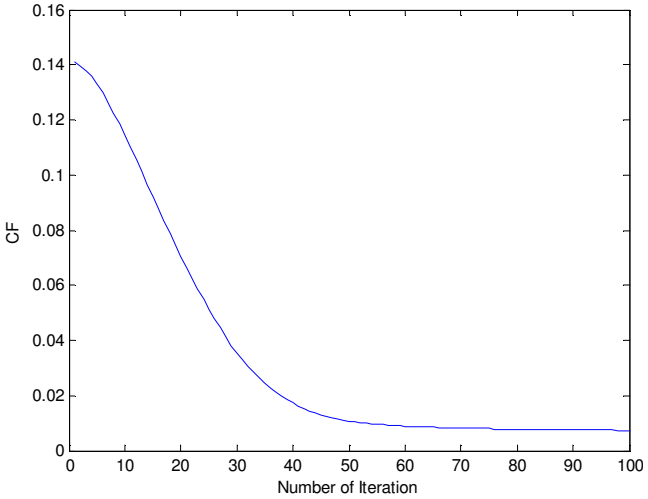

Fig. 8: Cost function versus the number of iterations.

V. VLC System Complexity

Significant SNR and 3dB channel enhancements can be achieved by introducing beam steering and computer generated holograms in VLC systems [17], however the implementation complexity increases. This complexity is associated with the resources and computational time (computing the SNR and time delay) required to identify the optimum location to steer the optical beam to. In this section we evaluate the efficiency of the proposed FCGHs by considering time complexity.

The nature of a function *T(m)* [34] can be used to measure the computational complexity of algorithms, for example a linear algorithm of input size m can induce a linear time complexity of *T(m) = O(m)*. A single pass implementation algorithm with complexity order of *O(m)* has an acceptable performance with a small value of m. However, a large value of m makes it too complex. The classical beam steering algorithm with computer generated holograms [17] can identify the optimum hologram by scanning all the areas underneath the best transmitter (see Fig. 4), which has similar properties as the "one-pass" style algorithms. Therefore, the time complexity of the classical computer generated holograms is linear and can be given *T(m) = O(m)*. Here m represents the total number of regions that should be covered for each transmitter. Significant SNR improvements can be achieved by increasing the value of m. However, the time complexity increases dramatically and this is due to the total number of holograms required, which is m. In contrast, the FCGHs is a recursive algorithm based on a D&C method, where the process used to find the optimum hologram is recursively broken down into a number of iterations S. For example, in the case of four iterations (S=4), then then the complexity can be given as [34]:

$$T(m) = ST\left(\frac{m}{64}\right) + Sj = ST\left(\frac{m}{j2^S}\right) + Sj =$$

$$log\left(\frac{m}{j}\right) T(1) + j\, log\left(\frac{m}{j}\right) = j\, log_2\left(\frac{m}{j}\right) \quad (6)$$

where j is the number of sub-problems (quadrants in our FCGHs). In each iteration the transmitter divides the stored holograms into four quadrants (i.e., j = 4). For instance, in the case of m=256 (number of regions underneath the transmitter), hence the number of holograms required for classical computer generated hologram is 256. Then the computation time required to identify the optimum holograms is 256 ms (If each SNR computation is carried out in 1 ms, based on typical processor). On the other hand, the computation time required to identify the optimum holograms in the FCGHs is 24 ms (based on equation 6).

VI. The Impact of Beam Steering Technique on Room Illumination

The main function of the RGB-LDs light units is to provide sufficient illumination according to ISO and European standards [23]. Therefore, to ensure the illumination is at an acceptable level we controlled the white light directed towards the receiver so that only a small amount of the RGB-LDs light is beam steered towards the receiver (20% of light of RGB-LDs unit), and the remaining light is used for illumination. We found that 20% achieves good performance in terms of the improvement in the achievable channel bandwidth and data rate while obeying the illumination standards with an acceptable change in illumination (i.e. the reduction in illumination is within the threshold level of European standards, which is 300 lx).

Fig. 9 shows the horizontal illumination distribution for the eight RGB-LDs units, the comparison is carried out for the illumination with and without beam steering when 20% of the beam power is steered, applied at LD1 (see Fig. 4 for RGB-LDs numbers and locations). The LD1, LD4, LD5 and LD8 light units were located at the room corners, and when beam steering of more than 20% is carried out at one of these light units, this led to reduced illumination in the room corners that is less than the acceptable threshold level (i.e. less than 300 lx). The minimum illumination in the corner without beam steering was 336 lx, as shown in Fig. 9. However, when beam steering was applied at one of the corner RGB-LDs units (worst case scenario) the illumination decreased, due to a part of the RGB-LDs' light being steered towards the receiver location (e.g. at 1m, 1m, 1m). The minimum illumination value of 20% beam steering was 300 lx. Therefore, we chose 20% beam steering as an acceptable value that kept the illumination at an acceptable level (300 lx) and improved the SNR. We emphasise that the beam steering technique is carried out at one RGB-LDs light unit, the unit nearest to the receiver location (the RGB-LDs that has been chosen by the STB), while the remaining RGB-LD light units (seven RGB-LD light units) operate normally. Note that steering light to a receiver, not only increases the received power, it more importantly reduces the delay spread by increasing the power received through the direct ray well beyond the power received through reflections.

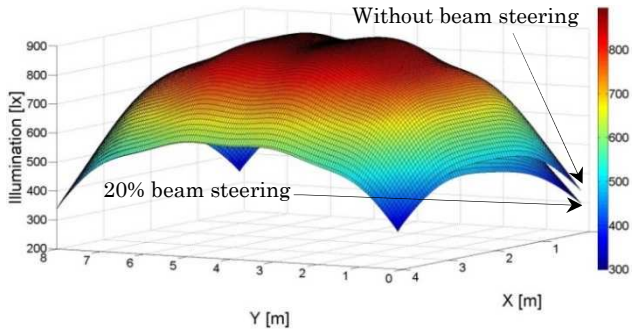

Fig. 9: The distribution of horizontal illumination on the communication floor without beam steering minimum illumination 336lx and maximum illumination 894lx, with 20% beam steering minimum illumination 300 lx and maximum illumination 889 lx.

VII. Simulation Results in an Empty Room

In this section, we evaluate the performance of the proposed fully adaptive ADR VLC system in an empty room in the presence of multipath dispersion and mobility. The

proposed system is examined in fourteen different locations when the receiver moves along the y-axis. The results are presented in terms of impulse response, delay spread, 3 dB channel bandwidth, SNR and BER. Due to the symmetry of the room, the results for x=1m equal the results for x=3m, therefore only x=1m and x=2m results are shown along the y-axis.

A. *Impulse responses*

The impulse responses of the two systems (DAT ADR LDs-VLC and fully adaptive ADR) at the room centre are depicted in Fig. 10. It can be seen that the fully adaptive ADR VLC's impulse response is better than that of the DAT ADR LDs-VLC in terms of received optical power. A significant increase in the received optical power can be achieved when the fully adaptive ADR replaces the DAT ADR LDs-VLC system. A factor of 4 improvement is achieved, from 4.6 µW to 18.64 µW. This significant improvement in the received power is due to steering a beam of white light towards the receiver location.

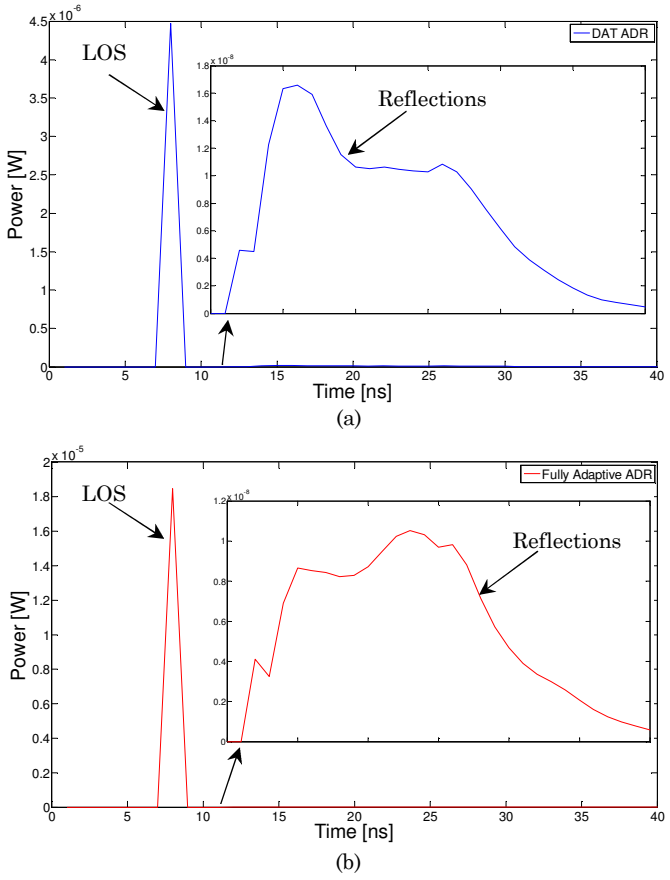

Fig. 10: Impulse responses of different VLC systems at room centre: (a) DAT ADR LDs-VLC and (b) Fully adaptive ADR VLC.

B. *Delay spread assessment*

Fig. 11 presents the communication system delay spread associated with the DAT ADR LDs-VLC and fully adaptive ADR VLC systems. The results show that the fully adaptive system has a lower delay spread than the DAT ADR LDs-VLC system at all the receiver locations considered. The delay spread for the DAT ADR system is relatively low (0.02 ns in the worst case) and this is attributed to two reasons: firstly, due to the narrow FOVs associated with each branch in the ADR, and this limitation in the FOV minimises the number of rays accepted. Secondly, DAT is used. However, to operate at high data rates (25 Gbps and beyond) the delay spread should be further reduced (i.e. less than 0.02 ns). The fully adaptive ADR system outperforms the DAT ADR system, as it dramatically decreases the delay spread from 0.02 ns to 0.0058 ns (by a factor of 3.4) at the room centre. The minimum communication channel bandwidth of the fully adaptive ADR was 26 GHz (where the delay spread is 0.0058 ns at points x=2m, y=2m, 4m, 6m). The significant increase in the channel bandwidth enables our proposed system to operate at higher data rates using a simple modulation technique, OOK [26]. Personick's analysis shows that the optimum receiver bandwidth is 0.7 times the bit rate [35]. For example, a 25 Gbps data rate requires a 17.5 GHz channel bandwidth. It should be observed that the performance of both systems is degraded at x=2m (high delay spread), and this can be attributed to the high ISI due to multipath propagation in the middle of the room (i.e. x=2m).

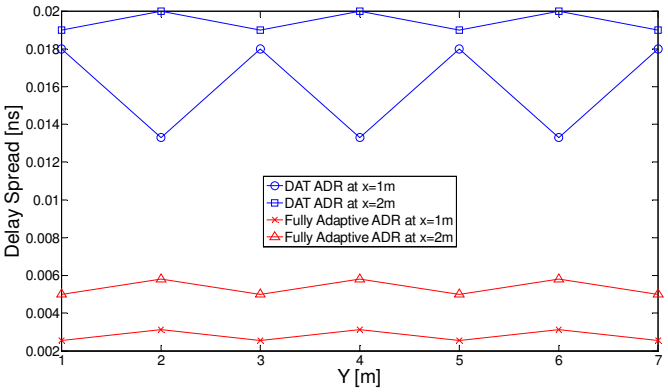

Fig. 11: Delay spread of two systems at x=1m, x=2m and along y-axis.

It should be noted that steering light to a receiver, not only increases the received power, it more importantly reduces the delay spread by increasing the power received through the direct ray well beyond the power received through reflections.

C. *3 dB channel bandwidth*

Previous work [15] has shown that DAT with an ADR can provide a 3 dB channel bandwidth of more than 8.3 GHz under the worst case scenario. However, the main problem with such a system is the low SNR. Therefore, to enable it to operate at 25 Gbps we proposed FCGHs to enhance the SNR and to utilize the significant increase in the channel bandwidth that will enable our proposed system (fully adaptive ADR VLC system) to operate at 25 Gbps. The 3 dB channel bandwidth at x=2m in our systems is shown in Table V. The results show that the proposed system has the ability to offer a communication channel with 3 dB bandwidth greater than 26 GHz.

Table V

CHANNEL BANDWIDTH OF THE PROPOSED SYSTEMS

System	3 dB channel Bandwidth [GHz]						
	Receiver Locations along the y-axis, Y [m]						
	1	2	3	4	5	6	7
DAT ADR	8.7	8.3	8.7	8.3	8.7	8.3	8.7
Fully Adaptive ADR	29.5	26	29.5	26	29.5	26	29.5

D. SNR

The VLC system's performance is best evaluated using the SNR, which gives due consideration to the noise and signal spread (eye opening). The probability of error is expressed as:

$$P_e = Q\left(\sqrt{SNR}\right) \tag{7}$$

where $Q(.)$ is the Gaussian function, approximated as:

$$Q(x) = \frac{1}{2} erfc\left(x/\sqrt{2}\right) \approx \frac{1}{\sqrt{2\pi}} \frac{e^{-\left(x/\sqrt{2}\right)^2}}{x} \tag{8}$$

The function has the value x=6 at probability of error of 10^{-9}. Hence, SNR=36 (15.6 dB) is needed for a 10^{-9} probability of error. In OOK the SNR associated with the received signal can be calculated by considering P_{s1} and P_{s0} (the powers associated to logic 1 and 0 respectively). These powers (P_{s1} and P_{s0}) determine the eye opening at the sample instant, thus ISI. The SNR is given by:

$$SNR = \left(\frac{R(P_{s1} - P_{s0})}{\sigma t}\right)^2 \tag{9}$$

where R is the receiver responsivity (0.4 A/W) and σ_t is the standard deviation of the total noise, that is the sum of shot noise, thermal noise and signal dependent noise. It can be calculated as:

$$\sigma t = \sqrt{\sigma_{shot}^2 + \sigma_{preamplifier}^2 + \sigma_{signal}^2} \tag{10}$$

where σ_{shot}^2 represents the background shot noise component, $\sigma_{preamplifier}^2$ represents the preamplifier noise component and σ_{signal}^2 represents the shot noise associated with the received signal. The PIN-HMET optical receiver proposed by Klepser [36] was used for the fully adaptive 25 Gbps ADR VLC system. The noise current spectral density for this preamplifier is 12 pA/√Hz and the preamplifier has a bandwidth of 18 GHz. In this study we considered SC method of processing the electrical signal from different branches in an ADR. In SC, the receiver simply selects the branch with the largest SNR among all the branches. The SNR_{SC} is given by [29]:

$$SNR_{SC} = Max_i \left(\frac{R(P_{s1} - P_{s0})_i}{\sigma t_i}\right)^2 \; 1 \le i \le j \tag{11}$$

where j represents the number of ADR branches (j=3 in our ADR).

It should be noted that the fully adaptive ADR system has the ability to provide SNR values higher than those associated with the DAT ADR system. The results in Fig. 12 are in agreement with the general observation made in Fig. 11. For instance, the DAT ADR system at x=2m and y=4m had a delay spread higher than other locations, which led to a decrease in SNR. Note the variation in SNR in tandem with the delay spread (see Fig. 11) due to the effects explained. The DAT ADR system does not have the ability to operate at 25 Gbps due to the impact of ISI and multipath propagation. However, these effects can be mitigated by employing fully adaptive ADR VLC. It can be noticed that for both systems the SNR can be lower when the receiver moves along x=2m. This is due to the larger distance between the receiver and transmitter.

Table VI presents the BER values corresponding to the achieved SNRs at 25 Gbps for the DAT ADR and fully adaptive ADR systems at the line x=2m (due to room symmetry, we calculated BER at 1 m to 4 m along the y-axis). It can clearly be seen that the fully adaptive ADR system has the best performance compared to the other systems. The highest value of BER in the fully adaptive ADR system is equal to 2.9×10^{-6}, and this value can provide a good communication link. Forward error correction coding (FEC) can be used to further reduce the BER from 10^{-6} to 10^{-9} in the proposed system.

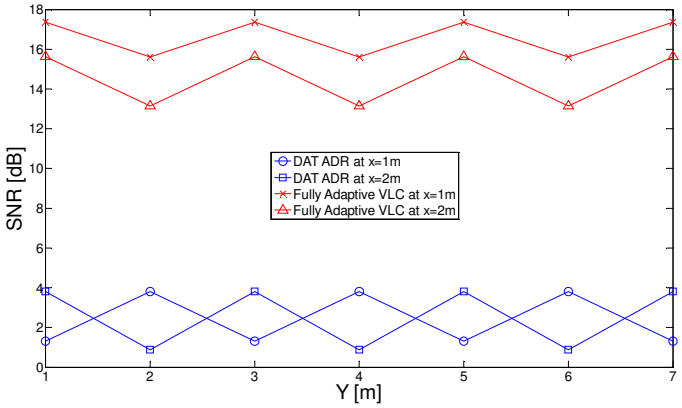

Fig. 12: SNR of two systems (DAT ADR and fully adaptive ADR) when operated at 25 Gbps at x=1m, x=2m and along the y-axis.

TABLE VI
BER PERFORMANCE OF THE PROPOSED SYSTEMS AT x=2m

System	BER			
	Receiver Locations along the y-axis, y [m]			
	1	2	3	4
DAT ADR	7.7×10^{-2}	10×10^{-1}	7.7×10^{-2}	10×10^{-1}
Fully Adaptive ADR	1.6×10^{-9}	2.9×10^{-6}	1.6×10^{-9}	2.9×10^{-6}

The system may choose to update its holograms less frequently even in the presence of mobility. This simplification is at the cost of an SNR penalty. In Fig. 13, the SNR penalty was calculated based on the old holograms settings while in motion. The results show the SNR penalty incurred as a result of mobility. The proposed system (fully adaptive ADR) design should allow a link margin. For

instance, with a link power margin of 3 dB, Fig. 13 shows that adaptation has to be done every time the receiver moves by ~1.4 m. If the SNR penalty is lower than 1 dB as desired in the proposed system, then Fig. 13 shows how often the system has to adapt its settings. For example, for the SNR penalty to be below 1 dB, the system has to adapt every 0.4 m, which corresponds to a 0.4 s adaptation rate. It should be noted that this adaptation has been done at the rate at which the environment changes and not at the system's bit rate.

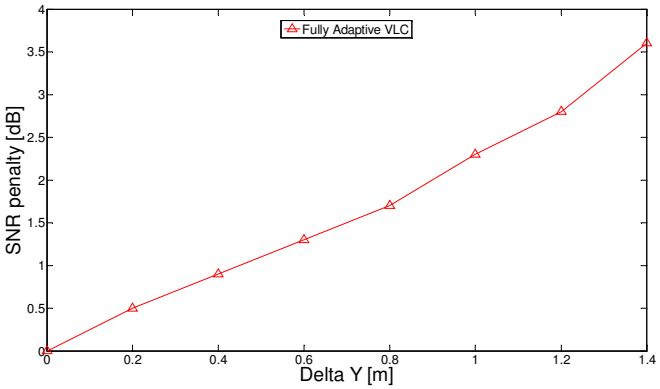

Fig. 13: SNR penalty of the proposed systems when the receiver moves from the optimum location at (2 m, 1 m, 1 m) along the y-axis.

VIII. Robustness To Shadowing, Signal Blockage and Mobility

In this section, we expand the analysis and the evaluation of the fully adaptive ADR system in realistic office arrangements where VLC signal blockage (as a result of mini-cubicles), doors and windows, furniture and multipath propagation all exist. The simulation was conducted in a room comparable to that used in Section II with an 8m × 4m × 3m room as an example. Fig. 14 shows the room arrangement. We considered a typical real indoor office. The room has a door, three large glass windows, a number of rectangular cubicles that have surfaces parallel to the walls of the room (physical partitions, which create shadowing) as well as other furniture such as filing cabinets, bookshelves and chairs. The ceiling has a diffuse reflectivity of 0.8, while the floor has a diffuse reflectivity of 0.3. The three glass windows and the door are assumed to not reflect any signal, thus their diffuse reflectivities are set at zero. In addition, the walls and the wall segments around the windows have diffuse reflectivity of 0.8. Two of the walls at x=4m and y=8m covered by filing cabinets and bookshelves, have a reflectivity of 0.4. It is assumed that signals that get to the office physical barriers (cubical office partitions) are blocked or absorbed. Additionally, chairs, desks and tables inside the room have a similar reflectivity to that of the floor (i.e. 0.3). The complexity is apparent in the room in Fig. 14 in which the physical partitions and the low reflective objects can create significant shadowing and VLC beam blocking as well as reduce the received optical power from reflections.

Comparisons are performed of the proposed system in two different environments (i.e., an empty room A and a realistic room B) when operating at 25 Gbps with full mobility. The results of the fully adaptive ADR VLC system were compared in rooms A (an empty room) and B (realistic room) in terms of impulse response, path loss and SNR. The proposed system is examined in fourteen different locations when the receiver moves along the y-axis.

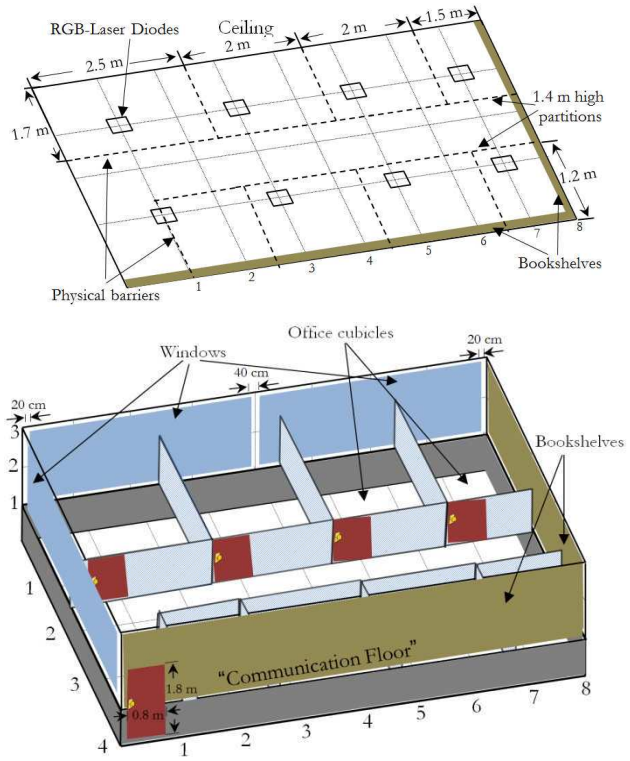

Fig. 14: Realistic room with a number of rectangular-shaped cubicles with surfaces parallel to the room walls, a door, three large glass windows and furniture, such as bookshelves and chairs.

A. *Impulse response*

Channel impulse responses at the room centre (i.e. x=2m and y=4m) for the fully adaptive ADR VLC system are shown in Fig. 15 for rooms A and B. It should be noted that both impulse responses of the proposed system are dominated by short initial impulses due to the LOS path between the transmitter and receiver. It can be clearly seen that the amount of received optical power from the reflections in room B is less than that received in room A, as shown in Fig. 15, and this is due to the existence of the door, windows, cubicles, partitions and bookshelves in room B that lead to reduced multipath propagation. These impulse responses suggest that the proposed system has good robustness against shadowing and mobility, and it has the ability to maintain LOS even in this harsh environment (i.e., room B), which is attributed to the FCGHs that maintain acceptable SNR in different environments. Although the received power from reflections was severely affected in room B, the LOS component remained the same in both room configurations in both systems, and the LOS component has the largest impact on the system performance. For instance, the power received by the proposed VLC system in room A was 18.64 μW, whereas it was 18.61 μW in room B, which indicates that the reduction in received power is negligible.

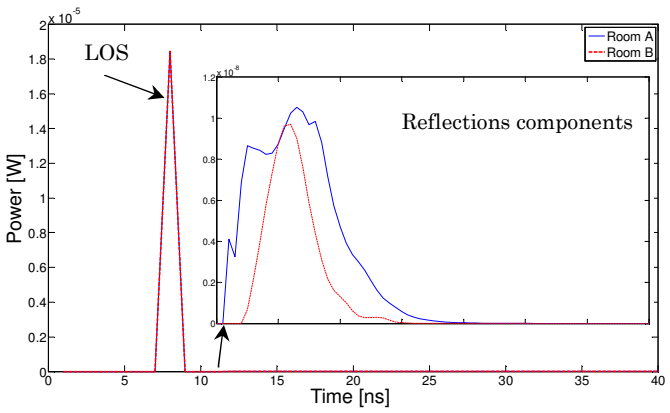

Fig. 15: Impulse responses of the fully adaptive ADR VLC system at room centre (2m, 4m, 1m) in two different environments (rooms A and B).

B. *Path loss*

Achieving high SNR at the receiver is one of the main targets of any communication system. The SNR in VLC systems is based on the ratio of the square of the received optical signal power and receiver noises [16]. Therefore, the average received optical power and path loss explain part of the main VLC system performance in the two different environments. Optical path loss can be defined as [37]:

$$PL(dB) = -10log_{10}(\int h(t)dt\,) \quad (12)$$

where $h(t)$ is the system impulse response. Fig. 16 shows the optical path loss of the proposed system in rooms A and B. It should be observed that the performance of the proposed system is comparable in rooms A and B, and this can be attributed to the LOS links available on the entire communication floor, which protects against shadowing and mobility in this system. It can be noticed that the path loss can be higher when the receiver moves along x= 2 m. This is due to the larger distance between the receiver and transmitter. Overall, the proposed system was evaluated and it was shown that it is able to achieve similar performance levels in an empty room and in a realistic indoor environment.

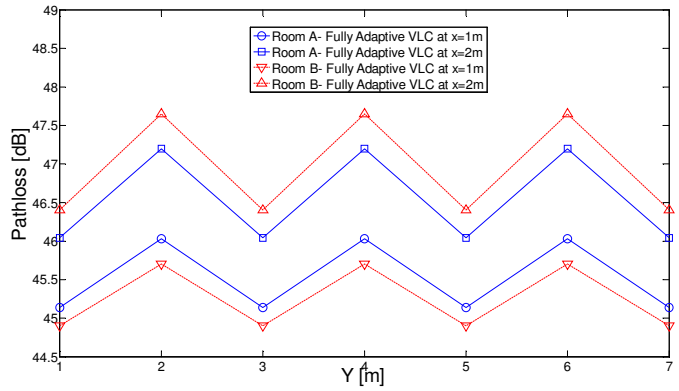

Fig. 16: Optical path loss distribution of the fully adaptive ADR VLC system in two different environments (rooms A and B) at x=1m and x=2m along y-axis.

C. *SNR*

Fig. 17 shows the SNR of the fully adaptive ADR VLC system at x=1m and x=2m along the y-axis over the communication floor for different environments (i.e. rooms A and B). In rooms A and B the proposed system has comparable results. There is very low degradation in the SNR when the proposed system operated in room B. This is attributed to the ability of our fully adaptive VLC system to adapt to such an environment. Also, it should be noted that the results in Fig. 17 are in agreement with the general observation made in Fig. 16. For instance, at the point x=2m and y=4m, the path loss is highest resulting in the lowest SNR.

Table VII shows the BER at 25 Gbps of the proposed system at line x=2m. It can be noted that in the realistic environment, the BER of the fully adaptive VLC system has increased slightly compared to an empty room. However, this increase does not severely affect the performance of the system; for example, the maximum value of BER provided by the proposed system is equal to 4.1×10^{-6}.

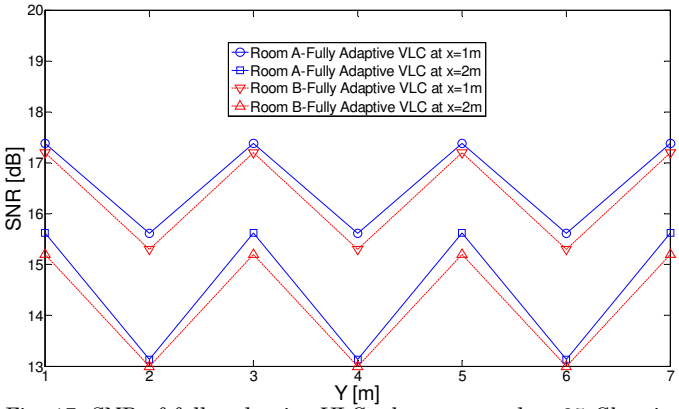

Fig. 17: SNR of fully adaptive VLC when operated at 25 Gbps in two different room scenarios at x=1m and at x=2m along the y-axis.

TABLE VII
BER PERFORMANCE OF THE PROPOSED SYSTEM AT x=2m IN DIFFERENT ENVIRONMENTS

System	BER			
	Receiver Locations along the y-axis, y [m]			
	1	2	3	4
Room A- Fully Adaptive VLC	1.6×10^{-9}	2.9×10^{-6}	1.6×10^{-9}	2.9×10^{-6}
Room B- Fully Adaptive VLC	4.4×10^{-9}	4.1×10^{-6}	4.4×10^{-9}	4.1×10^{-6}

IX. Conclusions

In this paper, we introduced a FCGHs VLC system and introduced a new fully adaptive VLC system that has ability to achieve 25 Gbps. In addition, DAT was introduced to FCGHs to reduce the effect of multipath dispersion, delay spread and increase the 3dB channel bandwidth and SNR when the system operates at high data rates.

Increasing the number of holograms / regions helps the transmitter accurately identify the receiver's location, hence improving the system performance. A search algorithm based on D&C was used in order to reduce the time needed to select the best pre-calculated hologram which leads to high SNR. The proposed system is coupled with an ADR to improve the received VLC signal in the presence of multipath dispersion, mobility, and shadowing.

The proposed FCGHs can effectively steer the VLC beam nearer to the receiver location at each given receiver location. It should be noted that the FCGHs are pre-calculated and stored in our proposed system without adding any complexity at the transmitter to reproduce (compute) the holograms. Thus the time required to find the optimum location to steer the beam to, was reduced from 224 ms to 32 ms. However, the total time required for efficient techniques (STB, FCGHs and DAT) is 112 ms. Therefore, the fully adaptive ADR VLC system can achieve 100% (25 Gbps) of the specified data rate when it is stationary, and 88.9% (22.2 Gbps) in the case of user movement, (user or object movement in the room).

The simulation results show that the fully adaptive ADR VLC system can significantly improve the impulse response, SNR, as well as the delay spread compared to DAT ADR VLC system. In addition, the proposed system can also adapt to environmental changes, offering a link that is robust against signal blockage and shadowing. The BER provided by our proposed system in realistic indoor environment is about 10^{-6} at 25 Gbps in the worst case scenario.

To the best of our knowledge, the data rates achieved by our proposed system (i.e. 25 Gbps for a stationary user and 22.2 Gbps for a mobile user) are the highest data rates to date for an indoor VLC system with a simple modulation format (OOK) and without the use of relatively complex wavelength division multiplexing approaches.

ACKNOWLEDGMENT

Ahmed Taha Hussein would like to acknowledge with thanks the Higher Committee for Education Development in Iraq (HCED), Ministry of Higher Education and Scientific Research in Iraq (MOHE) and the University of Mosul for finical support during his research.

REFERENCES

[1] A. T. Hussein, and J. M. H. Elmirghani, "A Survey of Optical and Terahertz (THz) Wireless Communication Systems," IEEE Communications Surveys & Tutorials, (to be submitted), 2015.

[2] GreenTouch, "Green Meter Research Study: Reducing the Net Energy Consumption in Communications Networks by up to 90% by 2020," A GreenTouch White Paper, Version 1, 2013, available: http// www.greentouch.org / uploads / documents /GreenTouch_Green_Meter_ Research_Study_26_June_2013.pdf. Last access date 25 March 2016.

[3] F. Haider, X. Gao, X.-H. You, Y. Yang, D. Yuan, H. M. Aggoune, H. Haas, S. Fletcher, and E. Hepsaydir, "Cellular architecture and key technologies for 5G wireless communication networks," IEEE Communications Magazine, vol.52, no.2, pp.122-130, 2014.

[4] N. Fujimoto, and H. Mochizuki, "477Mbit/s visible light transmission based on OOK-NRZ modulation using a single commercially available visible LED and a practical LED driver with a pre-emphasis circuit," in Proc Opt. Fibre Commun. Conf. Expo. Nat. Fibre Opt. Eng. Conf., 2013, pp. 1–3.

[5] D. Tsonev, H. Chun, S. Rajbhandari, J. McKendry, S. Videv, E. Gu, M. Haji, S. Watson, A. Kelly, G. Faulkner, M. Dawson, H. Haas, and D. O'Brien, "A 3-Gb/s Single-LED OFDM-Based Wireless VLC Link Using a Gallium Nitride μLED," IEEE Photonics Technology Letter, vol.26, no.7, pp.637–640, 2014.

[6] Y. Wang, X. Huang, L. Tao, J. Shi, and N. Chi, "4.5-Gb/s RGB-LED based WDM visible light communication system employing CAP modulation and RLS based adaptive equalization," Optics Express, vol.23, issue 10 pp.13626-13633, 2015.

[7] M. T. Alresheedi, and J.M.H. Elmirghani, "Performance evaluation of 5 Gbit/s and 10 Gbit/s mobile optical wireless systems employing beam angle and power adaptation with diversity receivers," IEEE Journal on Selected Areas in Communications, vol.29, no.6, pp.1328-1340, 2011.

[8] F. E. Alsaadi, and J. M. H. Elmirghani, "High-speed spot diffusing mobile optical wireless system employing beam angle and power adaptation and imaging receivers," Journal of Lightwave Technology, vol.28, no.16, pp.2191–2206, 2010.

[9] L. Wu, Z. Zhang and H. Liu, "Transmit Beamforming for MIMO Optical Wireless Communication Systems," Wireless Personal Communications, vol.78, issue 1, pp 615-628, 2014.

[10] S. Kim, and S. Kim, "Wireless optical energy transmission using optical beamforming," Optical Engineering, vol.2, no.4, pp.205-210, 2013.

[11] T. Komine, "Visible Light Wireless Communication and Its Fundamental," PhD, Dept. of Information & Computer Science, Keio University, 2005.

[12] Visible light communication system: Nakagawa Group, 2010; Available from: http://www.youtube.com/watch?v=QEh5f49LsB4. Last access date 25 March 2016.

[13] A. T. Hussein, and J.M.H. Elmirghani, "Mobile Multi-gigabit Visible Light Communication System Employing Laser Diodes, Imaging Receivers and Delay Adaptation Technique in Realistic Indoor Environment," Journal of Lightwave Technology, vol.33, no.15, pp.3293-3307 2015.

[14] A. T. Hussein, and J.M.H. Elmirghani, "High-Speed Indoor Visible Light Communication System Employing Laser Diodes and Angle Diversity Receivers," 17th International Conference in Transparent Optical Networks (ICTON), pp.1-6, 2015.

[15] A. T. Hussein, and J.M.H. Elmirghani, "Performance Evaluation of Multi-gigabit Indoor Visible Light Communication System," The 20th European Conference on Network and Optical Communications, (NOC), pp.1-6, 2015.

[16] A. T. Hussein, and J.M.H. Elmirghani, "10 Gbps Mobile Visible Light Communication System Employing Angle Diversity, Imaging Receivers and Relay Nodes," Journal of Optical Communications and Networking, vol.7, issue 8, pp.718–735, 2015.

[17] A. T. Hussein, M. T. Alresheedi and J. M. H. Elmirghani, "20 Gbps Mobile Indoor Visible Light Communication System Employing Beam Steering and Computer Generated Holograms," Journal of Lightwave Technology, vol.33, no.24, pp.5242-5260, 2015.

[18] F. R. Gfeller, and U. H. Bapst, "Wireless in-house data communication via diffuse infrared radiation," Proc. IEEE, vol.67, no.11, pp.1474-1486, 1979.

[19] P. A. Haigh, T. T. Son, E. Bentley, Z. Ghassemlooy, H. Le Minh and L. Chao, "Development of a Visible Light Communications System for Optical Wireless Local Area Networks," in Proc. IEEE Computing Communications and Applications Conference (ComComAp), pp.315-355, 2012.

[20] G. Cossu, A. M. Khalid, P. Choudhury, R. Corsini, and E. Ciaramella, "3.4 Gbit/s visible optical wireless transmission based on RGB LED," Optics express, vol.20, no.26, pp.501-506, 2012.

[21] T. Komine, and M. Nakagawa, "Fundamental analysis for visible-light communication system using LED lights," IEEE Transactions on Consumer Electronics, vol.50, no.1, pp.100-107, 2004.

[22] S. Soltic and A. Chalmers, "*Optimization of laser-based white light illuminants*," Optics express, vol.21, no.7, pp.8964-8971, 2013.

[23] "European standard EN 12464-1: Lighting of indoor work places", [online] Available:http://www.etaplighting.com/uploadedFiles/Downloadable_documentation/documentatie/EN12464_E_OK.pdf. Last access date 25 March 2016.

[24] A. Neumann, J. J. Wierer, W. Davis, Y. Ohno, S. Brueck, and J. Y. Tsao. "*Four-color laser white illuminant demonstrating high color-rendering quality*," Optics express, vol.19, no.104, pp.982-990, 2011.

[25] J. R. Barry, J. M. Kahn, W. J. Krause, E. A. Lee, and D. G. Messerschmitt, "Simulation of multipath impulse response for indoor wireless optical channels," IEEE Journal on Selected Areas in Communications, vol.11, no.22, pp.367-379, 1993.

[26] M. T. Alresheedi, and J.M.H. Elmirghani, "10 Gb/s Indoor Optical Wireless Systems Employing Beam Delay, Power, and Angle Adaptation Methods With Imaging Detection," Journal of Lightwave Technology, vol.30, no.12, pp.1843-1856, 2012.

[27] J. M. Kahn, and J.R. Barry, "Wireless infrared communications," Proceedings of the IEEE, vol.85, no.2, pp.265-298, 1997.

[28] A. G. Al-Ghamdi, and J.M.H. Elmirghani, "Analysis of diffuse optical wireless channels employing spot-diffusing techniques, diversity receivers, and combining schemes," IEEE Transactions on Communications, vol.52, no.10, pp.1622-1631, 2004.

[29] A. G. Al-Ghamdi, and J. M. H. Elmirghani, "Line strip spot-diffusing transmitter configuration for optical wireless systems influenced by background noise and multipath dispersion," IEEE Transactions on Communication, vol.52, no.1, pp.37-45, 2004.

[30] F. E. Alsaadi, and J.M.H. Elmirghani, "Adaptive mobile line strip multibeam MC-CDMA optical wireless system employing imaging detection in a real indoor environment," IEEE Journal on Selected Areas in Communications, vol.27, no.9, pp.1663-1675, 2009.

[31] F. E. Alsaadi, M. Nikkar, and J. M. H. Elmirghani, "Adaptive mobile optical wireless systems employing a beam clustering method, diversity detection, and relay nodes," IEEE Trans. Commun., vol.58, no.3, pp.869–879, 2010.

[32] M. Tolstrup, "Indoor Radio Planning: A Practical Guide for GSM, DCS, UMTS, HSPA and LTE," John Wiley & Sons., 2011.

[33] P. Viswanath, D. N. C. Tse, and R. Laroia, "Opportunistic beamforming using dumb antennas," in IEEE International Symposium on Information Theory, 2002.

[34] J. Kleinberg, and É. Tardos, "Algorithm design," Pearson Education India, 2006.

[35] S. D. Personick, "Receiver design for digital fiber optical communication system, I," Bell Syst. Tech. J., vol. 52, pp. 843–874, 1973.

[36] B. Klepser, J. Spicher, C. Bergamaschi, W. Patrick, and W. Bachtold, "High speed, monolithically integrated pin-HEMT photoreceiver fabricated on InP with a tunable bandwidth up to 22 GHz using a novel circuit design," Eighth International Conference on Indium Phosphide and Related Materials, IPRM, pp.443-446, 1996.

[37] A. G. Al-Ghamdi, and J.M.H. Elmirghani, "Performance comparison of LSMS and conventional diffuse and hybrid optical wireless techniques in a real indoor environment," IEE Proceedings Optoelectronics, vol.152, issue 4, pp.230-238, 2005.

Ahmed Taha Hussein received a B.Sc. (First Class Hons.) in electronic and electrical engineering from the University of Mosul, Iraq, in 2006 and an M.Sc. degree (with distinction) in communication systems from the University of Mosul, Iraq, in 2011. He is a Higher Committee for Education Developments in Iraq (HCED) Scholar and is currently working toward a Ph.D. degree in the school of Electronic and Electrical Engineering, University of Leeds, Leeds, UK.

Prior to his Ph.D. study, he worked as a Communication Instructor in Electronic and Electrical Engineering Department in the College of Engineering, University of Mosul, Iraq from 2006 to 2009. He also worked as a lecturer in the Electronic and Electrical Engineering Department in the College of Engineering, University of Mosul, Iraq from 2011 to 2012. He is the author of a number of published papers. His research interests include performance enhancement techniques for visible light communication systems, visible light communication system design and indoor visible light communication networking.

Mohammed Alresheedi received a B.Sc degree (with First Class Honor) in Electrical Engineering from King Saud University, Riyadh, Saudi Arabia, in 2006 and an MSc degree (with Distinction) in Communication Engineering from Leeds University, United Kingdom, in 2009. He received the Ph.D. degree in Electronic and Electrical Engineering from Leeds University, United Kingdom in 2014. He is currently an Assistant Professor in the Electrical Engineering Department, King Saud University. His research interests include adaptation techniques for OW, OW systems design, indoor OW networking and visible light communications.

Prof. Jaafar M. H. Elmirghani is the Director of the Institute of Integrated Information Systems within the School of Electronic and Electrical Engineering, University of Leeds, UK. He joined Leeds in 2007 and prior to that (2000–2007) as chair in optical communications at the University of Wales Swansea he founded, developed and directed the Institute of Advanced Telecommunications and the Technium Digital (TD), a technology incubator/spin-off hub. He has provided outstanding leadership in a number of large research projects at the IAT and TD. He received the Ph.D. in the synchronization of optical systems and optical receiver design from the University of Huddersfield UK in 1994 and the DSc in Communication Systems and Networks from University of Leeds, UK, in 2014. He has co-authored Photonic switching Technology: Systems and Networks, (Wiley) and has published over 400 papers. He has research interests in optical systems and networks. Prof. Elmirghani is Fellow of the IET, Fellow of the Institute of Physics and Senior Member of IEEE. He was Chairman of IEEE Comsoc Transmission Access and Optical Systems technical committee and was Chairman of IEEE Comsoc Signal Processing and Communications Electronics technical committee, and an editor of IEEE Communications Magazine. He was founding Chair of the Advanced Signal Processing for Communication Symposium which started at IEEE GLOBECOM'99 and has continued since at every ICC and GLOBECOM. Prof. Elmirghani was also founding Chair of the first

IEEE ICC/GLOBECOM optical symposium at GLOBECOM'00, the Future Photonic Network Technologies, Architectures and Protocols Symposium. He chaired this Symposium, which continues to date under different names. He was the founding chair of the first Green Track at ICC/GLOBECOM at GLOBECOM 2011, and is Chair of the IEEE Green ICT committee within the IEEE Technical Activities Board (TAB) Future Directions Committee (FDC), a pan IEEE Societies committee responsible for Green ICT activities across IEEE, 2012-present. He is and has been on the technical program committee of 34 IEEE ICC/GLOBECOM conferences between 1995 and 2015 including 15 times as Symposium Chair. He received the IEEE Communications Society Hal Sobol award, the IEEE Comsoc Chapter Achievement award for excellence in chapter activities (both in 2005), the University of Wales Swansea Outstanding Research Achievement Award, 2006, the IEEE Communications Society Signal Processing and Communication Electronics outstanding service award, 2009, a best paper award at IEEE ICC'2013, the IEEE Comsoc Transmission Access and Optical Systems outstanding Service award 2015 in recognition of "Leadership and Contributions to the Area of Green Communications" and received the GreenTouch 1000x award in 2015 for "pioneering research contributions to the field of energy efficiency in telecommunications". He is currently an editor of: IET Optoelectronics, Journal of Optical Communications, IEEE Communications Surveys and Tutorials and IEEE Journal on Selected Areas in Communications series on Green Communications and Networking. He is Co-Chair of the GreenTouch Wired, Core and Access Networks Working Group, an adviser to the Commonwealth Scholarship Commission, member of the Royal Society International Joint Projects Panel and member of the Engineering and Physical Sciences Research Council (EPSRC) College. He has been awarded in excess of £22 million in grants to date from EPSRC, the EU and industry and has held prestigious fellowships funded by the Royal Society and by BT. He is an IEEE Comsoc Distinguished Lecturer 2013-2016.